AD-A112 214 AEROSPACE CORP EL SEGUNDO CA SPACE SCIENCES LAB F/G 4/1
SOFT X-RAYS FROM THE SUNLIT EARTH'S ATMOSPHERE.(U)
FEB 82 D L MCKENZIE, H R RUGGE, P A CHARLES F04701-81-C-0082
UNCLASSIFIED TR-0082(2940-01)-6 NL

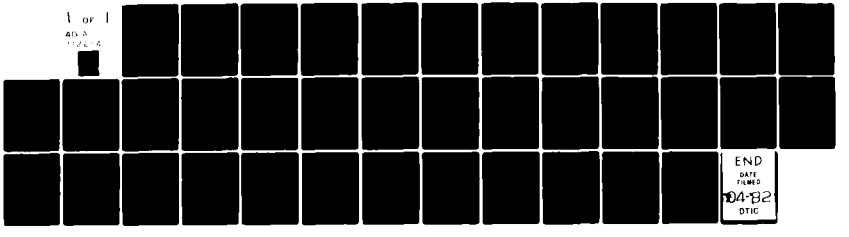

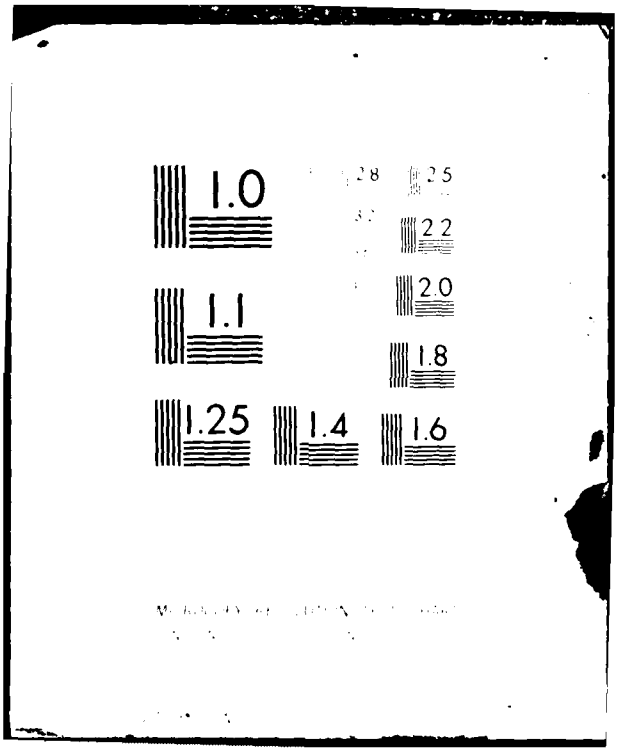
1.0
1.1
1.25
1.4
1.6
2.0
1.8
2.2

(12)

REPORT SD-TR-82-04

Soft X-Rays from the Sunlit Earth's Atmosphere

D. L. McKENZIE and H. R. RUGGE
Space Sciences Laboratory
Laboratory Operations
The Aerospace Corporation
El Segundo, Calif. 90245

and

P. A. CHARLES
University of California
Berkeley, Calif.

15 February 1982

APPROVED FOR PUBLIC RELEASE;
DISTRIBUTION UNLIMITED

Prepared for

SPACE DIVISION
AIR FORCE SYSTEMS COMMAND
Los Angeles Air Force Station
P.O. Box 92960, Worldway Postal Center
Los Angeles, Calif. 90009

This interim report was submitted by The Aerospace Corporation, El Segundo, CA 90245, under Contract No. F04701-81-C-0082 with the Space Division, Deputy for Technology, P.O. Box 92960, Worldway Postal Center, Los Angeles, CA 90009. It was reviewed and approved for The Aerospace Corporation by G. A. Paulikas, Director, Space Sciences Laboratory. Lt R. Weidenheimer, SD/YLVS, was the project officer for Mission-Oriented Investigation and Experimentation (MOIE) Programs.

This report has been reviewed by the Public Affairs Office (PAS) and is releasable to the National Technical Information Service (NTIS). At NTIS, it will be available to the general public, including foreign nations.

This technical report has been reviewed and is approved for publication. Publication of this report does not constitute Air Force approval of the report's findings or conclusions. It is published only for the exchange and stimulation of ideas.

Randall S. Weidenheimer, 2nd Lt, USAF
Project Officer

Florian P. Meinhardt, Lt Col, USAF
Director, Directorate of Advanced
Space Development

FOR THE COMMANDER

Norman W. Lee, Jr., Colonel, USAF
Deputy for Technology

UNCLASSIFIED

SECURITY CLASSIFICATION OF THIS PAGE (When Data Entered)

REPORT DOCUMENTATION PAGE		READ INSTRUCTIONS BEFORE COMPLETING FORM
1. REPORT NUMBER SD-TR-82-04	2. GOVT ACCESSION NO. AD-A112	3. RECIPIENT'S CATALOG NUMBER 214
4. TITLE (and Subtitle) SOFT X-RAYS FROM THE SUNLIT EARTH'S ATMOSPHERE		5. TYPE OF REPORT & PERIOD COVERED 6. PERFORMING ORG. REPORT NUMBER TR-0082(2940-01)-6
7. AUTHOR(s) David L. McKenzie, Hugo R. Rugge, and P. A. Charles		8. CONTRACT OR GRANT NUMBER(s) F04701-81-C-0082
9. PERFORMING ORGANIZATION NAME AND ADDRESS The Aerospace Corporation El Segundo, Calif. 90245		10. PROGRAM ELEMENT, PROJECT, TASK AREA & WORK UNIT NUMBERS
11. CONTROLLING OFFICE NAME AND ADDRESS Space Division Air Force Systems Command Los Angeles, Calif. 90009		12. REPORT DATE 15 February 1982 13. NUMBER OF PAGES 37
14. MONITORING AGENCY NAME & ADDRESS(if different from Controlling Office)		15. SECURITY CLASS. (of this report) Unclassified 15a. DECLASSIFICATION/DOWNGRADING SCHEDULE

16. DISTRIBUTION STATEMENT (of this Report)

Approved for public release; distribution unlimited

17. DISTRIBUTION STATEMENT (of the abstract entered in Block 20, if different from Report)

18. SUPPLEMENTARY NOTES

19. KEY WORDS (Continue on reverse side if necessary and identify by block number)

X-Rays
Solar X-Ray Albedo
Earth's Upper Atmosphere

20. ABSTRACT (Continue on reverse side if necessary and identify by block number)

The HEAO-1 A-2 experiment low-energy porportional counters, designed to investigate celestial X-ray sources, have been used here to measure the X-ray spectrum of the sunlit earth in the energy range 0.2-0.8 keV. The X-rays arise by coherent scattering of, or fluorescence of atmospheric constituents by, solar coronal X-rays incident on the atmosphere. Although the relative spectral contributions of the two processes depend upon the sun-earth-satellite geometry, fluorescent oxygen and nitrogen K X-ray emission is always important. The

DD FORM 1473 (FACSIMILE)

UNCLASSIFIED

SECURITY CLASSIFICATION OF THIS PAGE (When Data Entered)

19. KEY WORDS (Continued)

20. ABSTRACT (Continued)

observed spectra were compared with calculations in order to derive the coronal temperature and emission measure, parameters that characterize the incident solar spectrum. These derived parameters agree well with the expected values for the nonflaring sun, and good agreement was obtained between measurements closely spaced in time but having a wide range of geometries and counting rates. Thus X-ray observations of the sunlit earth's atmosphere can be a useful monitor of solar activity for satellite-borne instrumentation unable to view the sun directly. The total measured fluorescent line flux agreed well with calculations, but the N/O line ratio did not. This disagreement is attributed to several causes, including the relative weakness of N emission at high altitudes where fluorescence is particularly important, the presence of line emission in the solar spectrum, and possible small calibration errors. Since present detectors cannot resolve the O and N K X-rays, observation of X-ray fluorescence from the sunlit atmosphere will be useful in monitoring atmospheric constituents only to the extent that total line counting rates depend upon composition. X-rays from the sunlit earth are briefly examined as a source of background in auroral X-ray observations. During non-flare periods this background should be unimportant above about 2 keV.

PREFACE

The A-2 experiment on HEAO-1 is a collaboration lead by E. Boldt (Goddard Space Flight Center) and G. Garmire (Cal Tech) with collaborators at Goddard Space Flight Center, Cal Tech, Univ. of California, Berkeley, and the Jet Propulsion Laboratory. This work was supported at The Aerospace Corporation by NASA Contracts NAS8-33235 and NASW-3338, by the Aerospace Corporate Research Program, and by the U.S. Air Force Space Division Contract F04701-81-C-0082; and at the University of California, Berkeley, by NASA Contracts CIT 44-727600 and NAS 5-23315. We thank Mr. Lee A. Christopher for developing the computer programs used in the analysis.

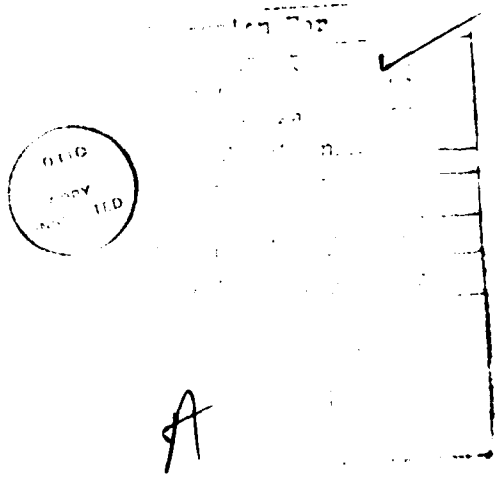

CONTENTS

FIGURES

TABLES

I. INTRODUCTION

The observations reported in this paper are the first satellite-based measurements of the characteristic Kα emission lines of nitrogen and oxygen from the earth's sunlit atmosphere. In addition to the atmospheric X-ray line emissions, lower energy X-ray emission was also observed. The two primary mechanisms for the production of X-rays from the sunlit atmosphere are the (coherent) Thomson scattering of solar X-rays from the electrons in the atomic and molecular constituents of the atmosphere and the absorption of incident solar X-radiation followed by the emission of characteristic K X-rays of nitrogen (0.392 keV), oxygen (0.525 keV), and argon (2.94 keV). Only a few observations of atmospheric X-rays produced by these mechanisms have been reported previously. A brief summary of early results from the experiment herein described has been published (RUGGE et al., 1979).

In 1967 HARRIES and FRANCEY (1968) observed atmospheric X-rays in the 2-5 keV region during two rocket flights. The X-rays were attributed to the above two production mechanisms, primarily on the basis of observed angular distributions (made with moderate angular resolution: 10° x 35° FWHM) which matched an approximate atmospheric scattering theory. Since these rocket experiments had effectively no energy resolution, they were unable to determine what, if any, contribution the fluorescently excited Ar K line made to the flux.

Also in 1967, GRADER et al., (1968) observed atmospheric X-rays with energies above 0.55 keV with a collimated proportional counter flown on a rocket. Collimation was ± 30° vertically and ± 5° horizontally. The authors attributed the radiation to oxygen and nitrogen K lines fluorescently excited by solar X-rays, based on the altitudes of observation (peak intensity was at 130 km) and the pulse-height distribution of the measured radiation. Although the threshold of the pulse height analyzer was above the K lines of O and N, the counter resolution was sufficiently broad that the pulse height distribution could be meaningfully compared to that which would be expected from the line radiation. Moderate agreement was found.

Recently, SEWARD et al. (1976) have observed the earth's atmosphere (in the 1.5-9 keV range) during solar flares using a proportional counter with an effective field of view of 5.2° (FWHM) on the Ariel V satellite. They observed the Ar K fluorescence line as well as a scattered solar component, apparently including solar X-ray line emission near 6.5 keV. Their observed Ar K X-ray flux was a factor of about 100 below that predicted by using an approximate calculation by AIKIN (1970).

While these reports have clearly established the existence of atmospheric X-rays resulting from solar X-rays striking the earth's atmosphere, they do not provide a basis for a complete understanding of the phenomenon. Indeed, the little theoretical work that has been done (AIKIN, 1970) is in substantial disagreement with the one measurement with which it meaningfully can be compared. Our intent in

this paper is to provide sufficient data and analysis so that a comprehensive understanding of these "earth-albedo" X-ray phenomena can be obtained. In Section II the exact theory is developed. Section III describes the observations made and the instrumentation used. Section IV presents an analysis of the data, and Section V summarizes the major points of the paper.

II. THEORY OF EARTH-ALBEDO X-RAYS

HARRIES and FRANCEY (1968) presented an approximate method for calculating the X-ray flux from a sunlit, planar, single-constituent atmosphere. Fluxes for both scattered and Ar K characteristic radiation were computed. When the approximation is extended to an atmosphere having a number of constituents, such as the earth's atmosphere, it gives satisfactory results in many cases. We will use the Harries and Francey approximation for some of the analysis in Section IV. AIKIN (1970) derived expected atmospheric X-ray intensities based on a presumably more complete theory. However, there was substantial disagreement between the predictions and the measurement of SEWARD et al. (1976). Unfortunately AIKIN's (1970) paper does not present enough detail to allow a check of his calculations to be made.

A complete and accurate theory, assuming fluorescence and coherent Thomson scattering of the incident solar X-rays, is conceptually straightforward. Because, in the relevant energy range, the absorption cross-section is much greater than the scattering cross-section, only single scatterings need be considered. Consider the

geometry in Figure 1. The vector $\underset{\sim}{L}$ lies in the yz plane and extends from the scattering point P to a detector outside the atmosphere, making an angle θ with the z axis, the local vertical. $\underset{\sim}{H}$, the vector from the sun to P, makes an angle ϕ with the z axis, as shown. It does not necessarily lie in the yz plane. Let the detector at distance L have a small rectangular field of view of α radians parallel to the projection of $\underset{\sim}{H}$ on the plane normal to $\underset{\sim}{L}$ (which is also the plane of the detector) and β in the perpendicular direction. The box at P, shown in the expanded view, has one face normal to $\underset{\sim}{L}$ of size $L\alpha$ by $L\beta$ ($L\alpha$ parallel to the projection of H on the face in question). The third dimension, parallel to $\underset{\sim}{L}$, is dL (i.e., $\sec\theta dz$).

A. Scattered X-Rays

We first consider the scattered flux. If the flux density per unit energy of solar photons incident on the atmosphere is dN_0/dE (photon - cm^{-2} - s^{-1} - keV^{-1}), then the flux through the top of the box (photon - s^{-1} - keV^{-1}) is

$$\frac{dF(z,E)}{dE} = \frac{dN_0(E)}{dE} \exp(-\tau_I(z,E))(L\beta)(\sec\theta dz)\sin\Psi, \qquad (1)$$

where Ψ is the scattering angle (the angle between $\underset{\sim}{H}$ and $\underset{\sim}{L}$), $\sec\theta dz = dL$, and

$$\tau_I(z,E) = \sum_i \sigma_i(E) \int_z^\infty \sec\phi' n_i(z')dz' \; . \qquad (2)$$

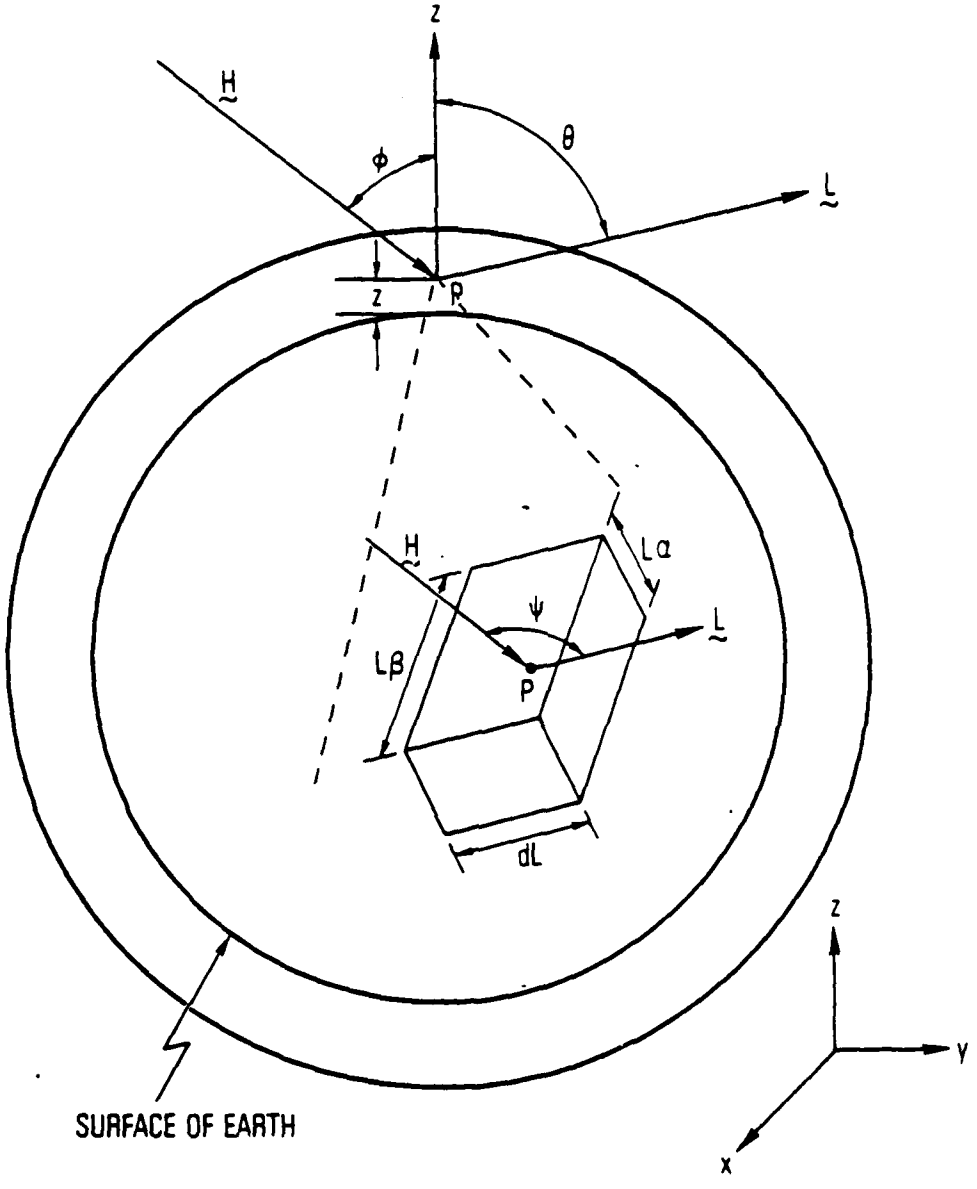

Figure 1. Geometry for a satellite observation of X-rays from the sun-lit earth's atmosphere. The interaction region is expanded at the center. $\underset{\sim}{H}$ is the vector from the sun to the interaction point, P, which is at an altitude z above the earth's surface. $\underset{\sim}{L}$ is the vector from P to the satellite, and the scattering angle Ψ is the angle between $\underset{\sim}{H}$ and $\underset{\sim}{L}$. The z axis passes through P and the center of the earth. The other symbols are explained in the text.

The angle ϕ' is, at each point on $\underset{\sim}{H}$, analogous to ϕ at P, $\sigma_i(E)$ is the total (absorption plus scattering) X-ray interaction cross-section (HENKE and SCHATTENBERG, 1975) for atmospheric constituent i, and z is the altitude at which the interaction occurs. The flux density at the detector (photon - cm^{-2} $-s^{-1}$ - keV^{-1}) arising from scatterings in the box is

$$\frac{dN_s(E)}{dE} = \frac{1}{L^2} \frac{dF(z,E)}{dE} \sum_i \left(\frac{d\sigma(E,\Psi)}{d\Omega}\right)_{s,i} n_i(z) e^{-\tau_0(z,E)} (L\alpha csc\Psi), \quad (3)$$

where $\left(\frac{d\sigma(E,\Psi)}{d\Omega}\right)_{s,i}$ is the differential cross-section for coherent scattering (COMPTON and ALLISON, 1935), and

$$\tau_0(z,E) = \sum_i \sigma_i(E) \int_z^{z_L} sec\theta' \, n_i(z')dz' \quad , \quad (4)$$

where z_L is the altitude of the detector. In equation (3) $L\alpha csc\Psi$ is the path length of the incident photon through the box. The total flux density is obtained by integrating equation (3) along the line of sight:

$$\frac{dN_s(E)}{dE} = \frac{dN_0(E)}{dE} \Omega_D sec\theta \sum_i \left[\left(\frac{d\sigma(E,\Psi)}{d\Omega}\right)_{s,i} \times \int_0^{z_L} n_i(z') \exp[-\tau_I(z',E) - \tau_0(z',E)] \, dz' \right] . \quad (5)$$

In writing equation (5) we have used the relationships $\Omega = \alpha\beta$ and $dL = \sec\theta dz$. Equation (5) holds for what we will call the "penetrating" case, the case wherein a backward extension of $\underset{\sim}{L}$ strikes the earth. For the other, the "grazing" case, one must integrate from ∞ to z_m and then from z_m to z_L, where z_m is the minimum z along the line of sight, $\underset{\sim}{L}$. The optical depths in equations (2) and (4) are evaluated by using the product of $n_i(z)$, the scale height of constituent i, H_i, and the Chapman integral (e.g., SMITH and SMITH 1972).

B. Fluorescent X-Rays

Fluorescently excited X-rays arise following absorption of incident X-rays having energy above $E_{K,j}$, the K absorption edge energy of the constituent, j, emitting the X-rays. The photon flux density, $N_{F,j}$ (photon - cm^{-2} - s^{-1}) is derived analogously to equation (5):

$$N_{F,j} = \frac{\Omega_D \, \omega_{K,j} \sec\theta}{4\pi} \times \tag{6}$$

$$\int_{E_{K,j}}^{\infty} \frac{dN_0(E)}{dE} \sigma_{K,j}(E) \int_0^{z_L} n_j(z') \exp[-\tau_I(z',E) - \tau_O(z',E_{F,j})] \, dz' \, dE.$$

In equation (6) $\sigma_{K,j}(E)$ is the cross-section for K shell photoelectric absorption; $\omega_{K,j}$, the K fluorescence yield of species j, is the fraction of K shell absorptions for which an X-ray rather than an Auger electron is emitted (TAWARA, et al., 1973); and $E_{F,j}$ is the energy of the emitted characteristic X-ray.

Equations (5) and (6) are not amenable to analytic solution. In some applications to be discussed below the expressions are too unwieldy to be handled by machine in a practical manner. Frequently in the grazing incidence case the approximation $\tau_I = \tau_O = 0$ is valid, and the equations can be readily calculated by computer. For the penetrating case we have extended the HARRIES and FRANCEY (1968) method for use with a multiple constituent atmosphere.

III. OBSERVATIONS

The observations described herein were made with the two low-energy detectors (LED) of the A-2 experiment flown on the HEAO-1 spacecraft launched in mid-August, 1977. The spacecraft and instrumentation were designed for observations of cosmic X-rays and gamma rays. The spacecraft rotates with a period of about 30 minutes about the sun-satellite vector $\underset{\sim}{H}$. Since $\underset{\sim}{L}$ is normal to $\underset{\sim}{H}$ (i.e. $\Psi = 90°$), the instruments scan the earth on almost every rotation, making possible the "accidental" observations described herein. The LEDs and the HEAO A-2 experiment are described by ROTHSCHILD et al. (1979). Basically, a single LED is a multi-anode, multi-layer, thin window, flow proportional counter with a multigrid collimator immediately in front of it. The collimator is designed so that, depending upon the use of certain sets of anodes, the detector field of view is either $2.95° \times 1.55°$ or $2.55° \times 2.80°$ ($\alpha \times \beta$). In the smaller field-of-view case the counter area is 194 cm^2, and in the larger FOV case it is 212 cm^2. The energy range of sensitivity is 0.15 - 3.0 keV, and spectral

analysis in this range is carried out by using a 32-channel pulse-height analyzer.

The 32-channel pulse-height analyzer used with the LEDs allows the individual channels to be narrower than the intrinsic resolution of the detectors. Hence spectral analysis is limited only by the detector resolution. We might expect to derive two kinds of information from the spectral data. First, we can determine the strengths of the two components of the radiation and thus the "fluorescence-to-scattering ratio". (It is tempting to call this the line-to-continuum ratio, but the scattered component consists largely of lines emitted in the solar corona.) This ratio, as a function of geometry, can be used as a check of the theory of X-ray emission from the sunlit atmosphere. Once the phenomena are understood, similar measurements can serve as a monitor of solar activity, in particular soft X-ray emission, for satellites (such as weather satellites) constrained to view the earth. Second, the ratio of N to O characteristic radiations might be used as a monitor of atmospheric composition. As will be seen below, this use is limited because the measured grazing incidence spectra, for which fluorescence is relatively strongest with respect to scattering, are heavily dominated by O emission, since atomic oxygen is abundant in the outer atmosphere and the detector efficiency is higher at 0.525 keV (O Kα) than at 0.392 keV (N Kα). Current detectors cannot resolve the O and N lines, and the small amount of N emission present has little effect on the observed spectrum.

The presence of fluorescent radiation is demonstrated in Figure 2, which shows the spectrum of a grazing observation (z_m, minimum z along $\underline{L}$, = 279 km) made on 17 August 1977. The error bars show the detector counting rates, and the solid curve shows the best-fit combined fluorescence and scattering spectrum. The χ^2 statistic for the fit was 7.97 for 9 degrees of freedom. The other two curves show the best fit fluorescent radiation spectrum (N/O count ratio was a fitting parameter) and scattering spectrum (solar coronal temperature T was a parameter) that add up to the solid line. The strong peak at 0.5 keV must arise from fluorescence; the solar spectrum cannot account for it. The peak in the scattered spectrum at 0.57 keV arises primarily from strong emission by the O VII ion in the corona, with a contribution from an O VIII line at 0.65 keV. There exists some uncertainty in the magnitude of this emission because of the uncertainty in the solar oxygen abundance and the high temperature sensitivity of the O VII emissivity below 2×10^6 K. This uncertainty can have some effect on the N/O line ratio derived from a spectrum, but the solar oxygen emission is small compared to the atmospheric fluorescence, so little error in the fluorescence/scattering ratio is introduced.

The measured X-ray intensity as a function of the sun-earth-satellite geometry gives one of the best tests of the albedo X-ray theory as well as providing a potential means of monitoring solar activity. The accurate HEAO-1 pointing and ephemeris determinations allow detailed atmosphere location (latitude, longitude, altitude, θ, ϕ, and z_m) to be obtained in a straightforward manner.

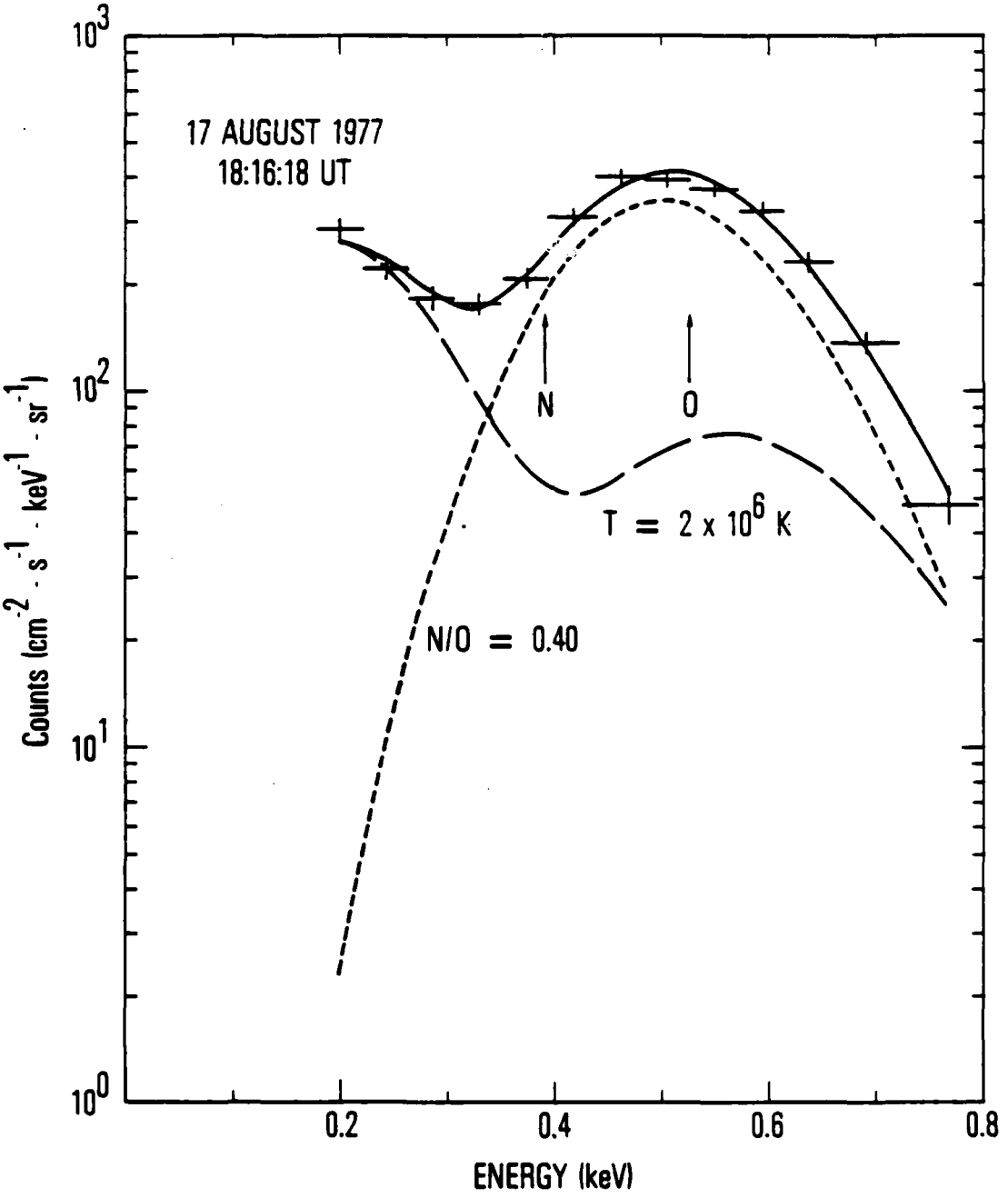

Figure 2. The X-ray spectrum of the sunlit earth for an observation with "grazing" geometry. The best-fit fluorescent line and scattering components are shown separately.

In Figure 3 the (energy) integrated albedo X-ray intensity (both scattered and fluorescent) is plotted as a function of time as the satellite scans the earth. HEAO-1 was at local noon near the middle of the plotted period so that the earth was viewed almost continuously during the 30-minute rotation period. The flux from the sunlit earth was about two orders of magnitude above the diffuse cosmic X-ray background. The times at which the instrument was viewing the earth's atmosphere rather than the sky are indicated in the figure ("occultation"). The symmetrical appearance of the two scans results from the unusual combination of the phase of the satellite rotation, the ratio of spin period and orbital period, and the occurrence of local noon at T ≈ 18 minutes.

A simplified model of the earth albedo X-ray flux is helpful in understanding the integrated counting rates in Figure 3. We have derived equations for the scattered and fluorescent X-ray flux densities from a plane, uniform, optically thick atmosphere. The derivations are similar to those for equations (5) and (6) and will not be given here. In many cases the plain, uniform, optically thick atmosphere is a useful approximation when proper account is taken of the composition at the height where most of the interactions occur. For scattering,

$$\frac{dN_s(E)}{dE} = \frac{dN_0(E)}{dE} \frac{\Omega_D}{(1 + \frac{\cos\theta}{\cos\phi})} \frac{\sum_i n_i (\frac{d\sigma(E,\Psi)}{d\Omega})_{s,i}}{\sum_i n_i \sigma(E)} \quad , \qquad (7)$$

and for fluorescence,

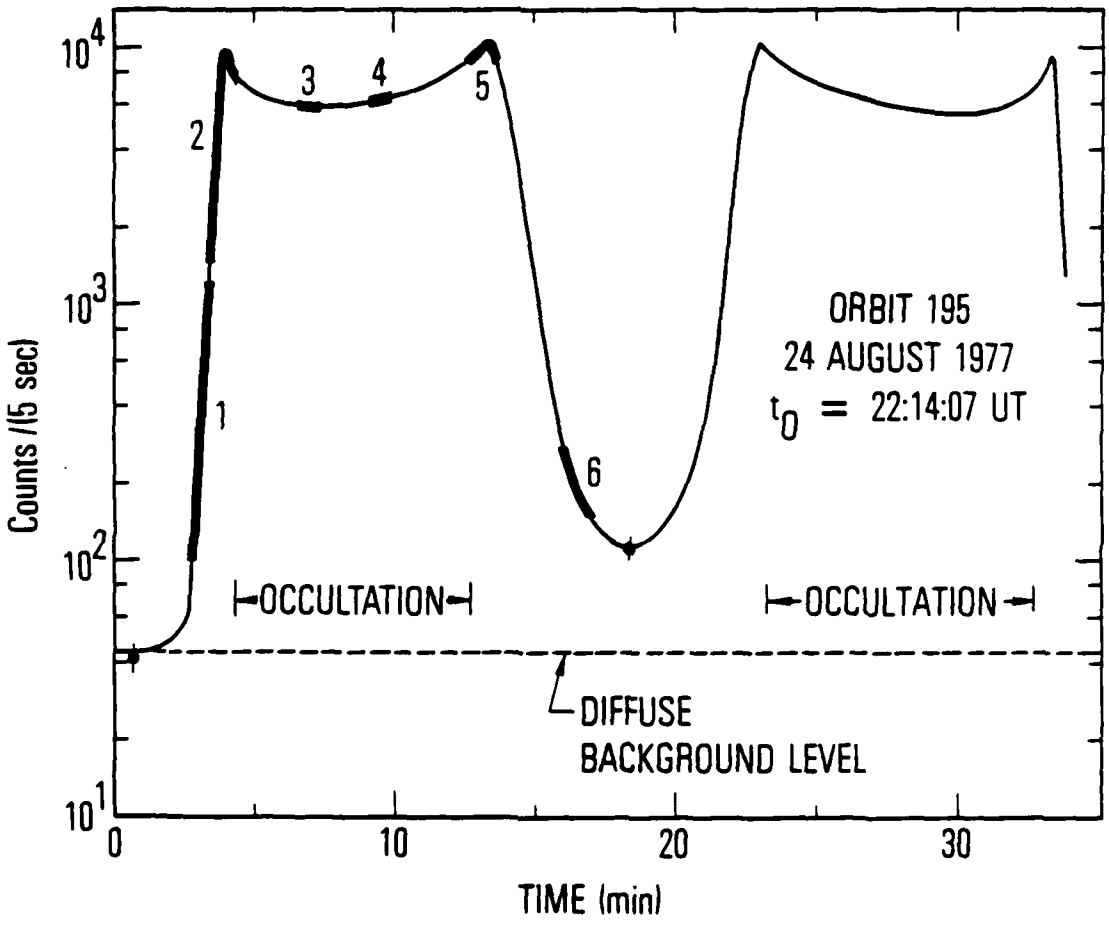

Figure 3. The total X-ray counting rate plotted as a function of time during two satellite scans across the sunlit earth. Local noon is at T = 18 minutes in the figure. The shaded portions are periods during which spectra were accumulated.

$$N_{F,j} = n_j \Omega_D \omega_{K,j} \int_{E_{K,j}}^{\infty} \left\{ \frac{(\sigma_{K,j}(E)/4\pi) \frac{dN_0(E)}{dE} dE}{\sum_i n_i \sigma_i(E) \left(\frac{\cos\theta}{\cos\phi} + \frac{\sigma_i(E_{F,j})}{\sigma_i(E)} \right)} \right\} , \qquad (8)$$

where the symbols are as previously defined. The behavior of n_i as a function of z can be approximated by the form $n_0 e^{-z/H(z)}$ where H(z) is the (local) scale height. For this reason, at least in the penetrating line of sight case, the bulk of the X-rays come from a narrow height range. The n_i in equations (7) and (8) must correspond to this interaction height. Note that the fluxes depend upon the relative concentrations of the atmospheric constituents rather than the absolute concentrations. This is because the model assumes that the atmosphere is optically thick. HARRIES and FRANCEY (1968) presented formulas similar to equations (7) and (8) for a single constituent atmosphere.

The curve in Figure 3 can be understood qualitatively in terms of equations (7) and (8). During the rapid rise starting at T = 2 minutes, $\theta = 90°$, but the optical depth of the atmosphere along the line of sight is not large; here the equations are invalid. The flux increase is due to the increase in optical depth. The peak at T = 4 minutes occurs because $\theta \approx 90°$ and the atmosphere is optically thick along this line of sight. The fluxes then decrease as the earth is scanned and θ decreases. During this period ϕ is also decreasing. Finally, at about T = 13 minutes, $\theta \approx 90°$ and the atmosphere is optically thick and a second maximum is reached. The small residual above the diffuse background near T = 18 minutes (local noon) arises from

the atmosphere at and above the satellite's height as the instrument views in a direction parallel to the earth's surface.

Figure 4 presents spectra acquired during the corresponding shaded periods in Figure 3. As we mentioned above, the relative importance of fluorescence in terms of counting rates is higher for the grazing observations ($\theta \approx 90°$). (A glance at Figure 2 will show that fluorescence is important in all these spectra.) Equations (7) and (8) are useful in understanding spectra 2-5. The solar spectrum is steep, so most of the fluorescent X-rays arise from incident photons having energies only slightly above $E_{K,j}$. The ratio $\sigma_j(E_{F,j})/\sigma_j(E)$ is therefore small and, for $i \neq j$, $\sigma_i(E_{F,j})/\sigma_i(E)$ is only slightly larger than 1. This means that the fluorescent component is more sensitive to $\cos\theta/\cos\phi$ than is the scattered component. Therefore, as θ approaches 90°, the *fluorescent radiation* increases relative to the scattered component. This is apparent in spectrum 5. In the optically thin limit, τ_I and τ_O approach zero, simplifying equations (5) and (6) somewhat. The relative importance of the two processes depends upon the cross-sections, the integrated amount of material along the line of sight, and the incident spectrum. Spectra 1 and 6 clearly show that N and O fluorescence in the sunlit earth's atmosphere are important even when the sun is not very active (the Ottawa 2800-MHz solar flux on 24 August 1977 was only 84 solar flux units -- Solar Geophysical Data, 397, part I).

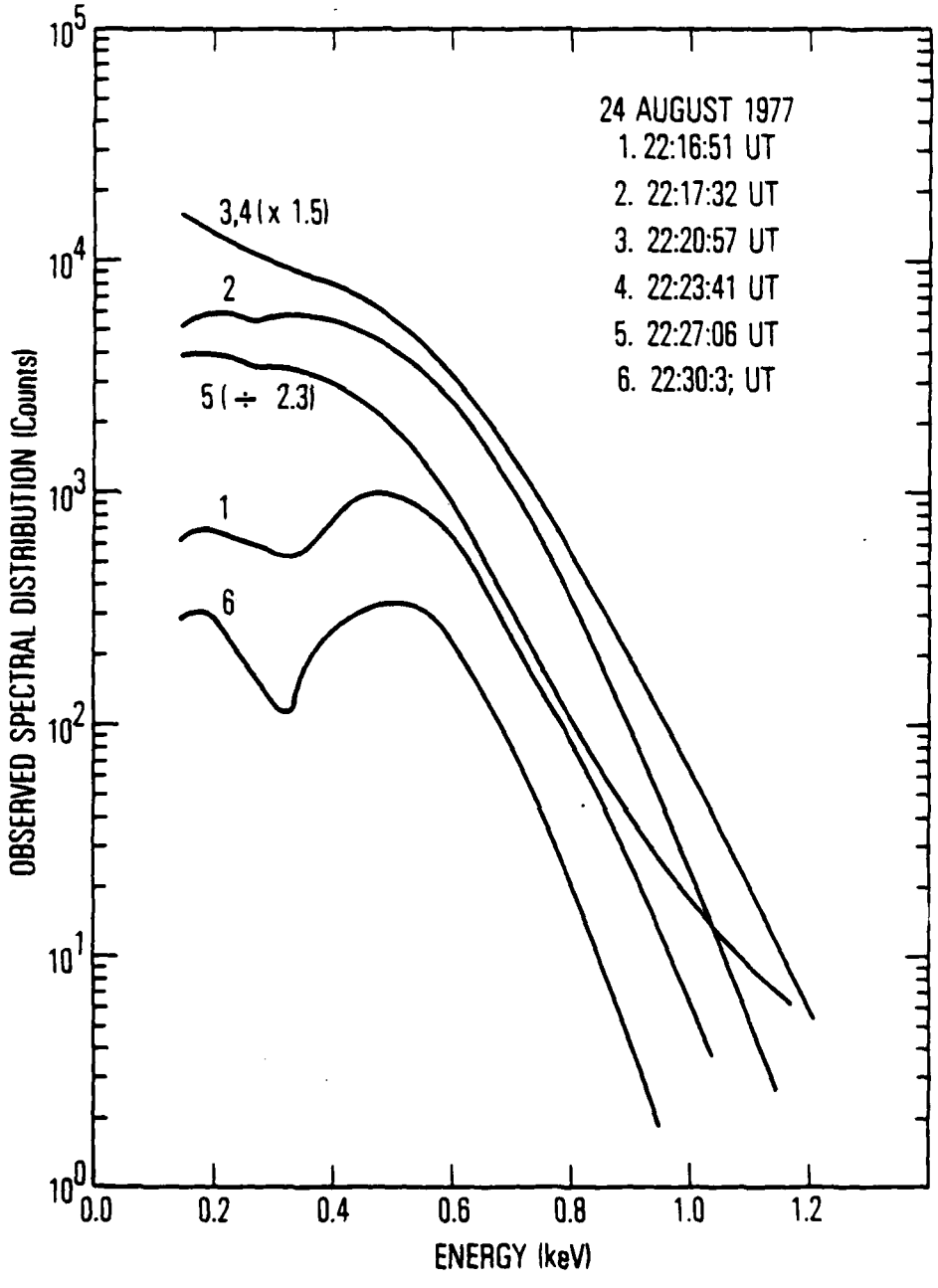

Figure 4. X-ray spectra of the sunlit earth's atmosphere. The importance of fluorescence in all of these spectra can be seen by comparing them with the steeply falling scattering spectrum in Figure 2.

IV. ANALYSIS

We have carried out the analysis of the X-ray data as follows. A computer program was used to obtain fits to the observed spectra with solar coronal temperature, emission measure (see below), total fluorescent line flux, and the ratio of N line counts to O line counts (hereafter, "N/O ratio") as fitting parameters. The X-ray spectrum incident upon the atmosphere was obtained from a solar X-ray spectrum model based on calculations by WALKER (1973), KATO (1976), and LOULERGUE and NUSSBAUMER (1973). The solar spectrum was then used with equations (6) and (8) and the CIRA 65 Atmospheric Model 5 at 12:00 hours to compute the fluorescence/scattering and N/O ratios. The computed ratios were then compared to the results from the best-fit program. A further check was obtained by comparing the parameters characterizing the solar spectrum derived from observations closely spaced in time but having very different geometries and hence different observed counting-rate spectra.

The X-ray spectrum of the (optically thin) solar corona has the form*

$$\phi(E,T) = CN_e^2 dV f(E,T) \ , \qquad (9)$$

*f may have minor N_e dependence, but in the present analysis this is unimportant.

where the emission arises from an element of volume dV at temperature T and having electron density N_e. In general the corona is not isothermal, but we have made the simplifying assumption that it is in deriving $dN_0(E)/dE$:

$$\frac{dN_0(E)}{dE} = [\int N_e^2 \, dV] \, f(E,T) \, . \qquad (10)$$

The integral in brackets is the emission measure, and the function f(E,T) is a complex combination of line and continuum emissions. In the energy range below a few hundred eV, where the scattering component is dominant, the solar spectrum is poorly known. Very few measurements have been made, and the uncertainties in the line emission are particularly large. Our computed spectrum in this region is based mostly on the calculations of KATO (1976).

The fitting program was implemented by computing, for each observation, the "scattering efficiency" ε_s (see equation (5)):

$$\varepsilon_s = \sec\theta \sum_i \left(\frac{d\sigma(E,\Psi)}{d\Omega}\right)_{s,i} \int_0^{Z_L} dz' n_i(z') \exp[-\tau_i(z',E) - \tau_0(z',E)]. \qquad (11)$$

(For grazing cases the integration limits were changed in accordance with the remark following equation (5).) The scattering part of the counting rate spectrum is then given by the product $\varepsilon_s \varepsilon_D A \Omega_D t \frac{dN_0(E)}{dE}$, where ε_D and A are the detector efficiency and area and t is the observing interval, 40.96 s. Because of the long observing interval and the satellite spin rate of 12°/minute, the geometry underwent con-

siderable change while each spectrum was accumulated. Therefore it was necessary to obtain an average ε_s by integrating over the observation period. The fitting program obtained best-fit emission measures and line strengths for each point on a grid of temperatures and N/O ratios. From these the best fits were chosen with a minimum χ^2 criterion.

In general the fits obtained were satisfactory. The best fit temperatures were almost always 1-2 x 10^6 K, in the range expected for the nonflaring corona (ACTON et al., 1972; MCKENZIE et al., 1978). Emission measures were 5-12 x 10^{49} cm^{-3} at 1 x 10^6 K and 2-9 x 10^{49} cm^{-3} at 1.5 x 10^6 K. While somewhat larger than the 1.5 x 10^{49} cm^{-3} obtained by ACTON et al. (1972) for the "general corona," excluding active regions (at 1.45 x 10^6 K), these values are not unreasonable when the active region contributions are considered. The fluorescence/scattering and N/O ratios will be discussed below. In many cases acceptable values of χ^2 were not obtained. In general, for the grazing observations where the counting rates were low and the statistics poor, acceptable values of χ^2 were obtained, but the penetrating cases, with good statistics, had high χ^2. This indicates that systematic errors were dominant. Possible sources of these errors would be lack of knowledge of the solar spectrum, failure of the isothermal solar corona assumption, and errors in the detector threshold, efficiency, or resolution calibration.

The fluorescence contribution was calculated by using equation (6) or (8). In the grazing cases equations (5) and (6) had to be used

and, because the effective height observed varied substantially during an observation, the equations had to be integrated over the changing field of view. The approximation $\tau_I = \tau_0 = 0$ was made to keep the integration from being too unwieldy. This is a good approximation; τ_I was small in all cases and, in the worst case treated, τ_0 did not exceed 0.32 at any energy.

For each analyzed spectrum the coronal emission measure as a function of coronal temperature was derived by comparing the calculated fluorescent flux with the observed fluorescence as determined by the best-fit program. The emission measure as a function of temperature was also determined by using the best-fit scattering spectrum at each temperature. These two curves are plotted in Figure 5 for four grazing observations on 17 August 1977. The derived emission measures are strongly dependent on temperature when fluorescence is used for the determination and weakly dependent when scattering is used. This is because f(E,T), the solar spectrum, contains a factor $e^{-E/kT}$ which has a strong temperature dependence for $E > 0.399$ keV, the minimum energy X-ray that can fluoresce nitrogen ($kT = 0.129$ keV for $T = 1.5 \times 10^6$ K). In contrast one can see from Figure 2 that scattered photons of energy below 0.3 keV have the greatest impact on the spectral fits. The curves in Figure 5 are closely spaced except for the earliest "scattering" curve. From the intersections of the curves we derive a coronal temperature of 1.1×10^6 K and emission measure of 7×10^{49} cm^{-3}. This temperature is below the best-fit temperature in most cases (see Figure 2), and χ^2 would lie in the range 2-3 per degree of

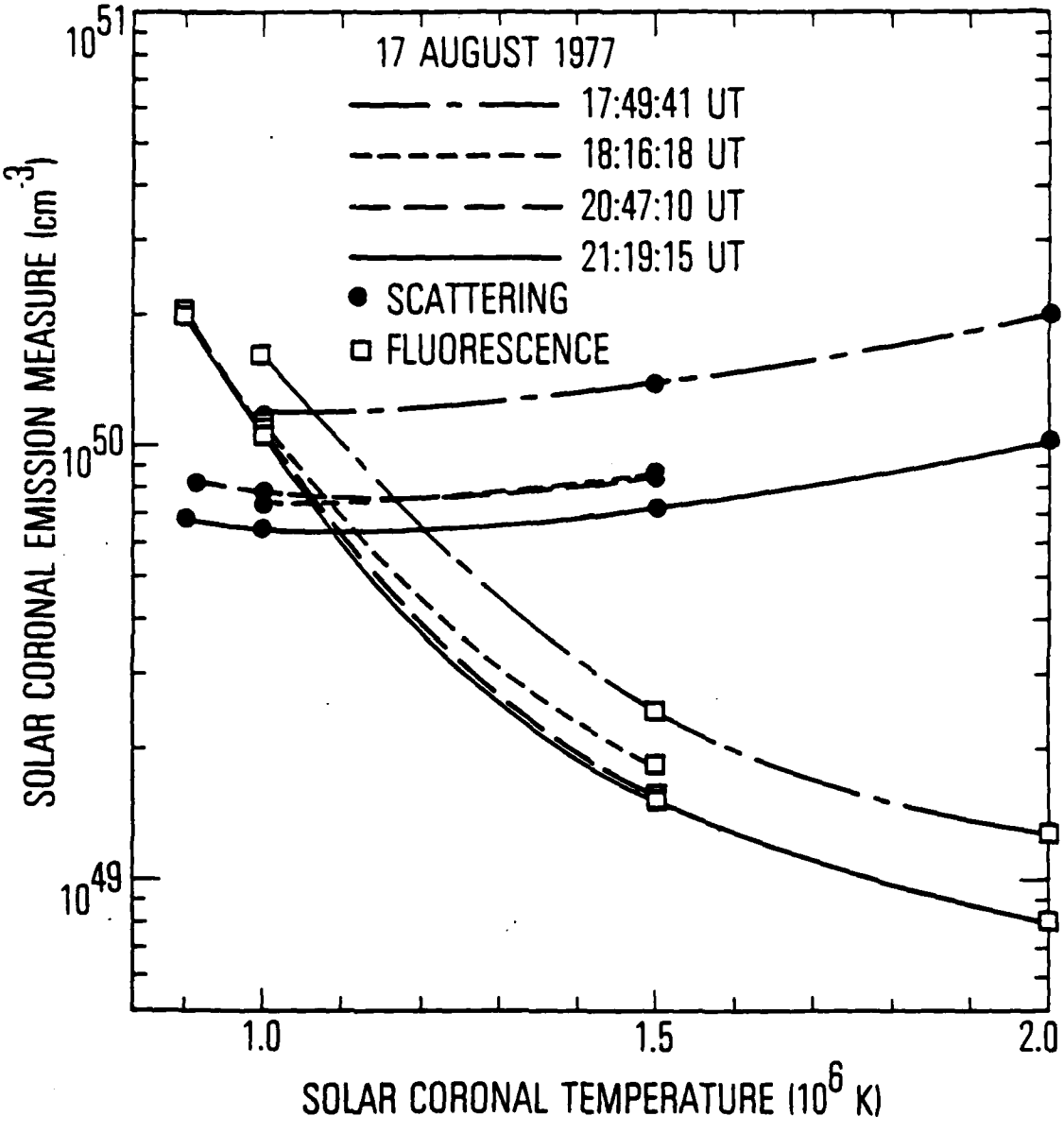

Figure 5. Derived solar coronal emission measure ($\int N_e^2$ dV) plotted as a function of coronal temperature. These two parameters were derived from fits to the calculated scattering and fluorescent contributions to the X-ray spectrum of the sunlit earth's atmosphere.

freedom. There is no apparent reason for the one outlying curve. All of the observations involved scans over a wide altitude range, typically 200-425 km. Interestingly, a solar subflare that peaked during the second observation was reported by a single observatory (Solar Geophysical Data, 397, part I). The flare had no soft X-ray emission that could be detected by observing the earth's atmosphere.

The N/O ratios determined from the best-fit program and from the integration of equation (6) are shown in Table 1. These are counting-rate ratios; the detector efficiency is taken into account. A range of fitted ratios is listed based on a 95% confidence interval derived by the method of CASH (1976). The calculated ratios are generally considerably smaller than the best-fit ratios. We have previously discussed possible reasons for this. In summary, for the grazing observations, combination of the fitting program with calculated fluorescent fluxes yielded a coronal temperature and emission measure in the expected range and fluorescent/scattering ratios consistent with observation. The calculated N/O ratios were smaller than the observed ones. This discrepancy probably arises from systematic errors that affect the fitting program.

For the optically thick observations the height at which most of the observed X-rays originated or were scattered did not change much during an observation. Therefore, the uniform plane atmosphere model (equation (8)) was used to compute the fluorescence and ϵ_s was not integrated over the changing field of view. The calculations were compared with the best-fit program results, and some observations for

Table 1. N/O counting-rate ratios

UT 17 Aug. 1977	N/O Ratio $T = 1.0 \times 10^6$ K		$T = 1.5 \times 10^6$ K	
	Fit	Calc.	Fit	Calc.
17:49:41	0.50	0.15	0.25-0.50	0.08
18:16:18	—	0.33	0.00-0.50	0.18
20:47:10	0.25-1.25	0.15	0.25-1.00	0.08
21:19:15	0.75-1.00	0.24	0.50-1.50	0.13

which integrated counting rates, but not spectra, were available were analyzed.

Spectra 3, 4 and 5 of Figure 3 were analyzed using the uniform plane atmosphere approximation. For each spectrum the N/O ratio, the emission measure, and the fluorescence/scattering ratio were determined from the fitting program and by calculation for T = 1.0 and 1.5 x 10^6 K. These results are plotted in Figure 6. The intersections of the graphs can be used to specify the plotted quantities. The coronal temperature and emission measure should be independent of geometry, and in fact the plots show little variation in either quantity. We found T = 0.9 - 1.4 x 10^6 K and emission measure = 7.5 x 10^{49} cm^{-3}. In addition an analysis similar to those in Figure 5 was done on spectrum 1 from Figure 3. We found T = 1.1 x 10^6 K and emission measure = 8 x 10^{49} cm^{-3}. These results agree very well with the plane atmosphere analysis. We point out that the fluorescence calculations depend upon the fluorescence yields ω_K, and that these are poorly known for O and N. For example, we use values of TAWARA et al. (1973), ω_{KN} = .00473 and ω_{KO} = .00645, while FINK et al. (1966) give ω_{KN} = .0015 and ω_{KO} = .0022. Figures 5 and 6 indicate that a change in ω_K would shift the "fluorescence" curves, resulting in a change in temperature but little change in emission measure at the intersections.

We have total counting rates, but not spectra, for a number of observations on 17 August 1977, around the time of the data in Figure 5. If temperature is fixed, emission measure can be derived from the

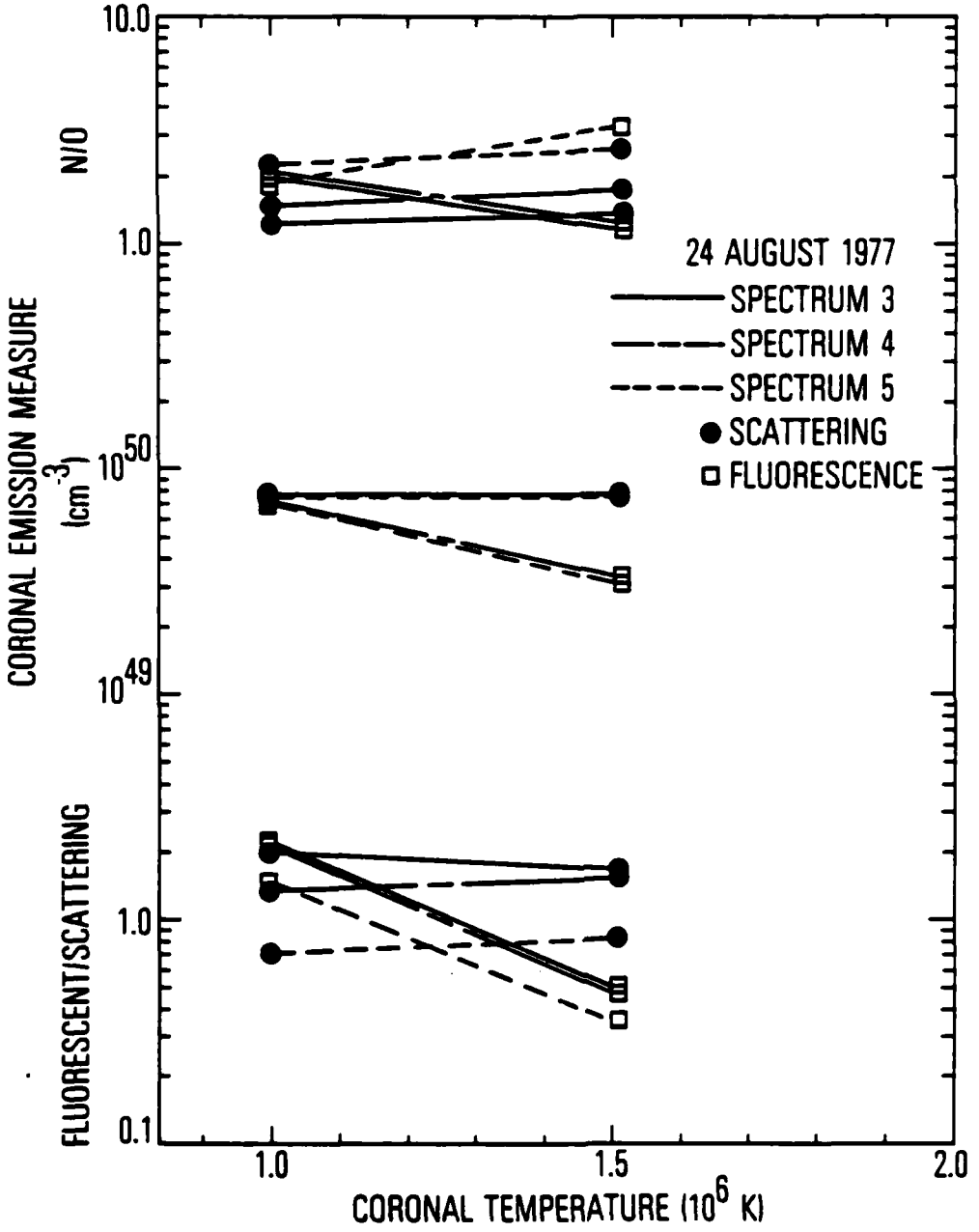

Figure 6. Nitrogen/oxygen line counting rate ratio, coronal emission measure, and fluorescent/scattering ratio plotted as a function of coronal X-ray temperature. The parameters were derived from fits of the observed X-ray spectrum to calculated model spectra.

observed counting rates and the plane atmosphere calculations. The results for such a calculation are shown in Table 2. For 1 x 10^6 K the emission measure is (6.4 ± 0.4) x 10^{49} cm^{-3}, and for 1.5 x 10^6 K it is (3.1 ± 0.4) x 10^{49} cm^{-3}. In Figure 5 we found T ≈ 1.1 x 10^6 K, and emission measure ≈ 7.5 x 10^{49} cm^{-3}. It is clear that the derived emission measure for the plane atmosphere calculations is somewhat smaller than that for the grazing observations. Nevertheless, at 1.0 x 10^6 K, near the temperature found for the grazing observations, the emission measures derived under the plane atmosphere approximation are tightly grouped for a wide variety of geometries. We conclude that the uniform plane atmosphere approximation is adequate for predicting the X-ray flux from the sunlit earth, provided that the region in the field of view is optically thick.

V. SUMMARY

We have analyzed a number of soft X-ray spectra of the sunlit earth obtained by the HEAO-1 A-2 experiment. The X-rays arise from coherent scattering of incident solar photons and fluorescence of atmospheric oxygen and nitrogen. The observations were compared with theoretical spectra discussed in Sections II, III and IV. Observations closely spaced in time but having a wide range of viewing geometries and counting rates were found to be consistent with similar incident solar X-ray spectra. The derived coronal temperatures and emission measures, parameters characterizing the solar spectrum, were in the range expected for the nonflaring sun (ACTON et al., 1972;

Table 2. Emission measures: plane atmosphere model

UT 17 Aug. 1977	θ (degrees)	φ (degrees)	Emission Measure 1.0×10^6 K	1.5×10^6 K
17:53:46	84.6	28.4	5.4 (49)	2.3 (49)
17:54:27	82.9	27.3	5.8 (49)	2.5 (49)
17:55:08	80.8	26.6	6.1 (49)	2.7 (49)
17:55:49	79.0	26.4	6.2 (49)	2.6 (49)
17:56:30	77.6	26.2	6.1 (49)	2.7 (49)
17:57:11	76.0	26.2	6.1 (49)	2.7 (49)
17:57:52	74.0	26.5	6.1 (49)	2.8 (49)
18:09:53	42.8	54.3	6.4 (49)	3.2 (49)
18:10:09	42.9	55.3	6.4 (49)	3.2 (49)
18:10:50	44.6	57.8	6.7 (49)	3.3 (49)
18:11:31	47.1	60.4	6.6 (49)	3.3 (49)
18:12:12	50.9	62.8	6.7 (49)	3.3 (49)
18:12:53	55.4	64.9	6.7 (49)	3.4 (49)
18:13:34	60.6	67.2	6.7 (49)	3.3 (49)
18:14:15	66.2	69.6	7.1 (49)	3.5 (49)
18:14:56	73.3	71.8	7.1 (49)	3.4 (49)
18:15:37	83.9	74.3	6.2 (49)	2.8 (49)

MCKENZIE et al., 1978). Therefore it appears that the sunlit earth's atmosphere can be used as a monitor of solar activity for satellites unable to view the sun directly.

All of the atmospheric spectra have a strong contribution from fluorescence. Because of this one might hope to monitor atmospheric composition by detecting characteristic X-rays, but this is apparently not practical. A major obstacle is the inability of proportional counters (which have the required large area and field of view) to resolve the O and N Kα lines. We have considered the use of gas-scintillation proportional counters, which have resolution approximately twice as good as that of a conventional proportional counter (e.g., ANDERSON et al., 1978), but for this purpose even this improved resolution is inadequate. Additional difficulties arise from strong oxygen line emission in the solar corona at energies near that of O Kα and from the dominance of atomic oxygen high in the earth's atmosphere where fluorescence is most evident (e.g., Fig. 4, Spectra 1 and 6). Remote sensing of fluorescent X-rays can be a useful monitor of atmospheric constituents only insofar as the total fluorescent line counting rate (which is predictable) depends upon composition.

X-rays from the sunlit earth constitute a background component that might interfere with, for example, satellite-based auroral X-ray observations. Indeed the data reported here were limited by the decision to turn the HEAO A-2 experiment off when viewing the earth, in order to avoid unnecessary detector fatigue. In a separate study, we have computed the X-ray spectrum from the sunlit earth during a period

of relatively high solar activity (but in the absence of flares), and compared it to measured auroral spectra (MIZERA et al., 1978). We found that even weak auroral emission should exceed the solar albedo flux at energies above about 2 keV, even with unfavorable geometry. At energies below 1 keV the solar albedo X-rays may cause difficulty, particularly for observations of weak aurorae. Little is known about the auroral X-ray spectrum at such low energies.

The A-2 experiment on HEAO-1 is a collaboration lead by E. Boldt (Goddard Space Flight Center) and G. Garmire (Cal Tech) with collaborators at Goddard Space Flight Center, Cal Tech, Univ. of California, Berkeley and the Jet Propulsion Laboratory. This work was supported at The Aerospace Corporation by NASA Contracts NAS8-33235 and NASW-3338, by the Aerospace Corporate Research Program and by the U. S. Air Force Space Division Contract F04701-79-C-0080 and at the University of California, Berkeley, by NASA Contracts CIT 44-727600 and NAS 5-23315. We thank Mr. Lee A. Christopher for developing the computer programs used in the analysis.

REFERENCES

ACTON, L. W., CATURA, R. C., MEYEROTT, A. J., WOLFSON, C. J., and CULHANE, J. L.	1972	Solar Phys. 26, 183.
AIKIN, A. C.	1970	Nature 227, 1334.
ANDERSON, D. F., KU, W. H.-M., NOVICK, R., and SCHENKMAN, M.	1978	I. E. E. E. Trans. Nuc. Sci. NS-25, 813.
COMPTON, A. H. and ALLISON, S. K.	1935	X-Rays in Theory and Experiment, D. Van Nostrand, Princeton, N. J., Chapter III.
FINK, R. W., JOPSON, R. C., MARK, H., and SWIFT, C. D.	1966	Rev. Mod. Phys. 38, 513.
GRADER, R. J., HILL, R. W., and SEWARD, F. J.	1968	J. Geophys. Res. 73, 7149.
HARRIES, J. R. and FRANCEY, R. J.	1968	Aust. J. Phys. 21, 715.
HENKE, B. L. and SCHATTENBERG, M. L.	1976	Advances in X-Ray Analysis 19, 749.
KATO, T.	1976	Ap. J. Supp. 30, 397.
LOULERGUE, M. and NUSSBAUMER, H.	1973	Astron. and Astrophys. 24, 209.
MCKENZIE, D. L., RUGGE, H. R., UNDERWOOD, J. H., and YOUNG, R. M.	1978	Ap. J. 221, 342.
MIZERA, P. F., LUHMANN, J. G., KOLASINSKI, W. A., and BLAKE, J. B.	1978	J. Geophys. Res. 83, 5573.
ROTHSCHILD, R., BOLDT, E., HOLT, S., SERLEMITSOS, P., GARMIRE, G., AGRAWAL, P., RIEGLER, G., BOWYER, S., and LAMPTON, M.	1979	Space Sci. Inst. 4, 269.
RUGGE, H. R., MCKENZIE, D. L., and CHARLES, P. A.	1979	Space Research XIX, 243.

SEWARD, F. D., HORTON, B., POLLARD, G., and SANFORD, P. W. 1976 Nature 264, 421.

SMITH, F. L., III, and SMITH, C. 1972 J. Geophys. Res. 77, 3592.

TAWARA, H., HARRISON, K. G., and DE HEER, F. J. 1973 Physica, 63, 351.

U. S. DEPT. of COMMERCE 1977 Solar Geophysical Data 397, Part I, 6, 10.

Reference is made to the following unpublished material:

WALKER, A. B. C., Jr. 1973 X-ray spectrum calculations.

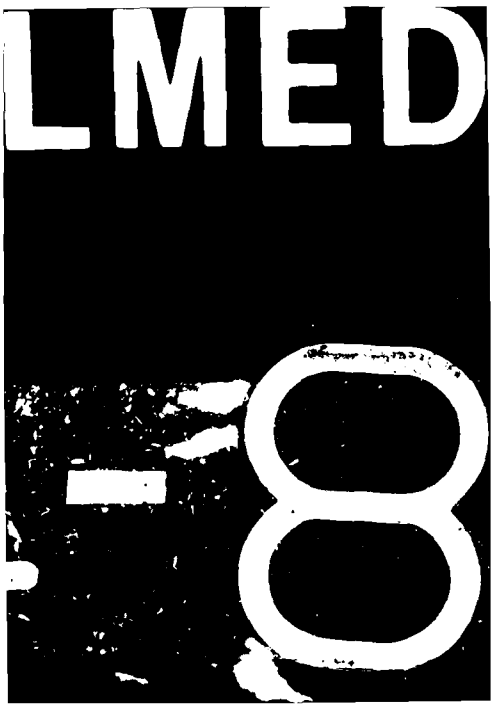
LMED
8